GeoInformatica
https://doi.org/10.1007/s10707-025-00547-x

RESEARCH

Spatiotemporal characterisation of underwater noise through semantic trajectories

Giulia Rovinelli[1] · Davide Rocchesso[2] · Marta Simeoni[1,3] · Esteban Zimányi[4] · Alessandra Raffaetà[1]

Received: 11 November 2024 / Revised: 17 March 2025 / Accepted: 22 April 2025

Abstract

Underwater noise pollution from human activities, particularly shipping, has been recognised as a serious threat to marine life. The sound generated by vessels can have various adverse effects on fish and aquatic ecosystems in general. In this setting, the estimation and analysis of the underwater noise produced by vessels is an important challenge for the preservation of the marine environment. In this paper we propose a model for the spatiotemporal characterisation of the underwater noise generated by vessels. The approach is based on the reconstruction of the vessels' trajectories from Automatic Identification System (AIS) data and on their deployment in a spatiotemporal database. Trajectories are enriched with semantic information like the acoustic characteristics of the vessels' engines or the activity performed by the vessels. We define a model for underwater noise propagation and use the trajectories' information to infer how noise propagates in the area of interest. We develop our approach for the case study of the fishery activities in the Northern Adriatic Sea, an area of the Mediterranean Sea which is well known to be highly exploited. We implement our approach using MobilityDB, an open source geospatial trajectory data management and analysis platform, which offers spatiotemporal operators and indices improving the efficiency of our system. We use this platform to conduct various analyses of the underwater noise generated in the Northern Adriatic Sea, aiming at estimating the impact of fishing activities on underwater noise pollution and at demonstrating the flexibility and expressiveness of our approach.

✉ Giulia Rovinelli
giulia.rovinelli@unive.it

Davide Rocchesso
davide.rocchesso@unimi.it

Marta Simeoni
simeoni@unive.it

Esteban Zimányi
esteban.zimanyi@ulb.be

Alessandra Raffaetà
raffaeta@unive.it

1 Ca' Foscari University of Venice, Venice, Italy

2 Università degli studi di Milano Statale, Milano, Italy

3 European Centre for Living Technology (ECLT), Venice, Italy

4 Université libre de Bruxelles, Brussels, Belgium

Published online: 19 May 2025

Keywords Semantic trajectories · Underwater noise · Fisheries · Spatiotemporal databases

1 Introduction

Underwater noise generated by human activities, especially from shipping, is known to produce short- and long-term effects on marine animal species. This noise pollution can disrupt the natural acoustic environment, leading to several adverse consequences. Some of the negative impacts include interference with communication, changes in behaviour, stranding, and increased mortality rates [1, 2]. Therefore, characterising underwater noise in a specific area is crucial for monitoring the health of aquatic life, assessing potential risks, and providing valuable information to ecologists and policymakers. This enables the development of effective strategies to maintain a productive and healthy ecosystem.

However, measuring underwater noise is a complex and resource-intensive task. It necessitates the use of hydrophones (underwater microphones) and requires a team of experts for deployment and calibration. Once the data has been collected, it must be processed and analysed to extract valuable insights. Additionally, there is the need to estimate underwater noise in areas where data collection is impractical or to extend coverage beyond what the hydrophones can monitor. Many approaches in the literature rely on acoustic models generated through numerical simulations to predict sound levels in the target area (see e.g. [3–5]). These models simulate sound propagation by accounting for reflection, diffraction, and absorption phenomena. They require precise input data and significant computational resources to create accurate acoustic maps. Typically, these models consider various environmental variables (like sea temperature, wind, waves, and salinity), detailed bathymetric information, and sound speed profiles at different depths. They may also incorporate Automatic Identification System (AIS) data to track vessel movements and include their noise emissions in the simulations.

In this paper, we follow a complementary approach that avoids using numerical simulation and fully relies on AIS data to calculate the underwater noise generated by vessels in space and time. Similar approaches in the literature are e.g., Erbe et al. [6] and Neenan et al. [7], where the authors' main goal is to readily provide noise maps of the area of interest. However, rather than developing an ad-hoc analysis for a specific case study, our aim is to propose a conceptual framework for underwater noise characterisation that can be easily instantiated on any sea area and can be used as a quick and effective means to monitor the noise pollution.

Our framework is based on semantic trajectories [8, 9]. Starting from AIS data, we reconstruct the vessel trajectories and deploy them in a spatiotemporal database. These trajectories are enhanced with semantic information, such as the acoustic characteristics of the vessels' engines and the activities conducted along their paths, which are then used to infer how the noise spreads in the area of interest.

To showcase the potential of the approach we consider the fishing activities of the Northern Adriatic Sea, which is known to be one of the most exploited areas of the Mediterranean Sea, so the underwater noise pollution is certainly among the effects of the intensive fishery activity. We build on our previous work [10, 11], which describes and implements a spatiotemporal database of the fishing activities in the Northern Adriatic Sea, and on a preliminary underwater noise model presented in Rovinelli et al. [12]. The trajectories of the fishing vessels are reconstructed starting from the AIS data, sent by ships and received by ground stations on the Italian coast. The dataset considered in this paper comprises all AIS data of the Italian and Croatian fishing vessels for the year 2020. In order to determine the acoustic characteristics of the vessels' engines and fine tune the propagation model, we take advantage of the direct

acoustic measurements produced by the Interreg project SOUNDSCAPE [13] that carried out an acoustic monitoring in the Northern Adriatic Sea from March 2020 to June 2021.

To estimate the generated noise, we define a model for underwater sound propagation and instantiate it by considering four different frequencies. We present the theoretical laws governing the underwater sound propagation and we also describe how we obtain the estimation for source sound levels, propagation loss and ambient noise, necessary for the definition of the model. We then use the spatiotemporal database to calculate the noise produced along the vessel trajectories. The sea area is partitioned into a regular grid composed of square spatial cells ($1km \times 1km$) which are enriched with environmental features such as sea surface temperature, sea salinity, and pH. Instead of using physical listening points (hydrophones), we treat the centroid of each cell as a *virtual* listening point where we calculate the received sound level.

The conceptual framework has been implemented in MobilityDB [14], an open-source platform for managing and analysing geospatial trajectory data. We use this platform to conduct various analyses that aim at estimating the impact of fishing activities on underwater noise pollution and at demonstrating the flexibility and expressivity of our approach. We first investigate the underwater noise generated by fishing activities at different frequencies. Then we look into the effects of the COVID-19 in the Northern Adriatic Sea, by comparing the underwater sound pressure levels in two periods, April and June 2020, i.e., during, and after the lockdown imposed in Italy. We also examine how fishing activity varies throughout the days of the week, focusing our analysis on the most intense fishing days - Monday to Thursday. Finally, we show that our tool allows for the visualisation of the underwater noise dynamics for a set of vessels chosen by the user according to several criteria.

The new contributions of this work w.r.t. the preliminary version presented in Rovinelli et al. [12] are the following:

- The underwater noise propagation model has been refined w.r.t. three main aspects. First, we integrate the contribution of speed in the computation of the source level of ships. In fact, as noted in [15], speed can influence the broadband source level of ships. Second, the transmission loss is no longer modelled simply by a spherical spreading law, but it is implemented as a combination between spherical propagation and mode stripping following [16]. This allows us to take into consideration the bathymetry of the study basin. Third, the ambient noise is no longer a constant value; it is computed using the exceedance level L_{90} [17], which represents the sound level exceeded 90% of the time. As mentioned in [18], L_{90} can be referred to as common natural acoustic conditions.
- We instantiate the refined model by considering not only the frequency of 63 Hz but also of 125 Hz, 400 Hz and 4000 Hz. The frequencies of 63 Hz and 125 Hz are the ones established as standard frequencies by the *European Marine Strategy Framework Directive* (MSFD) while 400 Hz and 4000 Hz allow us to show the increasing significance of environmental factors at higher ranges. For each frequency we calibrated the model parameters, specifically the source level of the ships, the ambient noise, the increment due to fishing and the transition range between spherical and mode stripping. The four considered frequencies provide a comprehensive view of the impact of fishing activities in the Northern Adriatic Sea.
- We propose an improved algorithm for calculating the noise level induced by the vessels. This new algorithm is based on the refined model of noise propagation and it is parametric with respect to the frequency of interest.

- The MobilityDB implementation has been enhanced by extensively exploiting the temporal types and spatiotemporal operations offered by MobilityDB. The result is a more compact and efficient code, leading to better execution times.
- We use the improved underwater noise propagation model and implementation to conduct several new analyses illustrating the impact of the fishing activities on underwater noise pollution in the Northern Adriatic Sea. These are only a few examples of the analyses that can be performed using the spatiotemporal database we have created.

The paper is organised as follows. Section 2 presents the literature on underwater noise characterisation. Section 3 details the data sources used in this study. Section 4 describes our model for the underwater sound propagation. Section 5 outlines the trajectory reconstruction and enrichment, the creation of a spatiotemporal database by means of MobilityDB and the description of the algorithm computing the underwater noise maps. Section 6 presents some analyses conducted on the obtained spatiotemporal database and some notes on model validation. Finally, some closing remarks are outlined in Section 7.

2 Related work

Underwater noise arising from human activities is known to have various adverse effects on aquatic life. These can range from acute effects such as permanent or temporary hearing impairment to chronic effects such as developmental deficiencies and physiological stress [1, 2]. As a general study, we mention the work by Cruz et al. [19] that summarised the status of European waters regarding continuous underwater radiated noise from shipping. The goal was to provide recommendations on possible future activities. The work focused on four main topics: characteristics and quantification of noise sources from various ship types, impacts on marine fauna, existing policies, including guidelines, decisions, resolutions and regulations and mitigation measures for the abatement of ship noise and noise-related impact.

The specific topic of interest in this paper, i.e. underwater noise generated by (fishing) vessels, has been explored by various authors in the literature. Below, we review some relevant contributions classified into three categories: (i) works relying on direct underwater noise measurements, (ii) approaches based on acoustic models obtained by numerical simulation, and (iii) proposals - like ours - that use only AIS data along with a sound propagation model.

2.1 Underwater noise characterisation by direct measurements

Some works in the literature address the issue of underwater noise data acquisition, transmission and storage. The most interesting one in our perspective is the dataset produced by the SOUNDSCAPE project [13], which carried out an acoustic monitoring of the Northern Adriatic Sea from March 2020 to June 2021. Nine monitoring stations were set up that encompass different environmental characteristics. Two datasets have been released, composed of 20 and 60 seconds averaged sound pressure level (SPL) data in a wide range of frequencies collected at the nine stations. SPL is the level of the root-mean-square sound pressure expressed in decibel, relative to a reference value of 1μPa [20]. These datasets are available on Zenodo [21] and the whole process of data acquisition, storing and post-processing is described by Petrizzo et al. in [22]. Furthermore, Picciulin et al. [18] perform some analyses and describe the spatial and temporal variations of the sound pressure levels recorded by the SOUNDSCAPE project during the monitoring period.

Other approaches propose methods for acoustic real-time measurements and monitoring, such as Diviacco et al. [23] and Moran et al. [24]. Differently, Farcas et al. [25] carried out

multi-site measurements to validate a large-scale shipping noise map constructed using a generic shipping noise model. Finally, the work by Picciulin et al. [26] shows two acoustic surveys conducted at 40 listening points distributed along the three inlets that connect the Venice lagoon to the sea, in order to characterise the local noise levels and evaluate the fish spatial distribution by means of its sounds.

2.2 Approaches based on numerical simulation

Most of the approaches to underwater noise characterisation are based on acoustic models obtained by numerical simulation to predict the sound levels in the area of interest. They simulate sound propagation taking into consideration reflection, diffraction and absorption phenomena and require precise information in input and a relevant computational effort (in terms of time and resources) to produce the acoustic maps of the area of interest. Such models usually account for many environmental variables (e.g. sea temperature, wind, waves, salinity), precise bathymetry information and sound speed profiles, possibly at different sea depths. They use AIS data to derive the vessels' trajectories and include their emitted sound into the model. The results obtained are often validated through real acoustic data measured on specific sites.

As a first approach in this category, we mention the work by MacGillivray et al. [3]. The authors present an acoustic model to predict anthropogenic sound levels at the Great Barrier Reef Marine Park in Australia. The model uses AIS data and wind speed data to simulate the time-dependent noise field in the area of interest and for the frequencies 64 kHz and 375 kHz. The model uses three months of AIS data and assign acoustic source levels to each vessel according to predefined values already calculated for the various vessels categories. The model includes environmental parameters such as ocean temperature and salinity as well as bathymetry information. The obtained results were compared against real data collected by an acoustic recorder placed on a specific site in the same period.

A similar approach is used by Larayedh et al. [4] to investigate the shipping noise in the Red Sea for the frequency band 40-100 Hz. The acoustic model, based on simulation, includes two months of AIS data belonging to specific categories of shipping vessels (tankers, bulkers, container ships, open hatch vessels and vehicle carriers), whose sound levels were derived from [27]. Bathymetry data, sea temperature and salinity are included, as well as spatial and temporal sound speed profiles specifically calculated for the Red Sea. The authors emphasise the computational effort needed to calculate the resulting maps of predicted noise levels, which required the use of a supercomputer. Results include the maps of predicted spectral noise level (averaged over the considered frequency band) for a specific day at different depths, and maps considering the two months under exam.

Along the same line, Ghezzo et al. present in [5] a numerical reconstruction of the sound field in the Northern Adriatic Sea basin for the year 2020. Acoustic modelling was performed by the Quonops© [28] underwater noise prediction system, which is based on simulation. *Natural Sound Maps* were produced by taking into account the sound propagation properties of the local environment (hourly wind and waves data, daily mean sea temperature and salinity, bathymetry data). Additionally, a combination of natural sources and AIS-based marine traffic were used to produce the *Baseline Sound Maps*. The AIS dataset included all types of vessels and the source level noise produced by the various categories of vessels were derived from [27]. The trawling activity of the fishing vessels was taken into account to consider an increased noise level when the trawler is in use. Calibration of the AIS-based model was performed using the SOUNDSCAPE [13] measured data. The authors present annual Baseline sound maps and excess 20 dB sound maps for the frequencies 63 Hz, 125 Hz

and 250 Hz. The study included specific analyses on protected areas of the Northern Adriatic Sea.

The work by Ghezzo et al. [5] is very relevant to our study as it examines the same area (the Northern Adriatic Sea), period (2020), and source of ground truth data (the SOUNDSCAPE time series measurements) as well as some common frequencies (63 Hz and 125 Hz), while adopting a different approach (ours falls under the category of "Approaches Based on AIS Data" described in the next subsection). Unfortunately, the results of the two studies cannot be directly compared. In fact, since we currently have access only to AIS data from fishing vessels, our results are based solely on this data whereas Ghezzo et al. consider the AIS data of all types of vessels. Moreover, it is important to note that our primary goal is different from [5]: we aim to provide a flexible tool for performing, with reduced computational effort, a number of various analyses, not limited to the generation of noise maps. This is made possible by the creation of a spatiotemporal database which stores semantically enriched vessel trajectories.

2.3 Approaches based on AIS data

Other proposals in the literature avoid the use of numerical simulation and give a more simplified description of the sound propagation effects. They are based on AIS data and they usually adopt a sound propagation model to calculate the transmission loss in the area of interest. The goal is to readily provide acoustic maps that can be used by policymakers for a first quantitative spatiotemporal underwater noise evaluation. They are computationally efficient, even for large datasets.

As a first approach in this setting, we mention the one by Erbe et al. [6] that uses the ship transits derived from AIS data and provided by the Canadian Guard Coast. The authors apply a sound propagation model to derive a cumulative large-scale noise map of the area of interest for the frequency band 10-2000 Hz. The authors include a comparison with field measurements. Similarly, Neenan et al. [7] develop a vessel noise modelling method using AIS data and online data on estimated source levels of individual ships. The authors divide the area of interest into a spatial grid of 1×1 km and consider a single frequency of 80 Hz. They calculate the propagation loss in a 5 km ray around each vessel's position taking into account also sediment type and bathymetry. The goal is to produce heatmaps of average received sound levels over monthly periods.

The approach followed in this paper is similar to that in [6, 7] since we also use AIS data and a model of sound propagation to derive a spatiotemporal characterisation of the underwater noise of the area of interest. However, the main goal of the works [6] and [7] is to produce cumulative noise maps. Instead, in our approach, cumulative noise maps are only one of the possible outputs. The two key features that distinguish our approach are the use of semantic trajectories and their deployment into a spatiotemporal database. Semantic trajectories enable the association of semantic information with trajectories, like the activities performed by a vessel during the trip. The spatiotemporal database allows for answering any query about underwater noise at different temporal and spatial granularities, with the possibility of considering any set of vessels. For example, a user can visualise the noise produced by a single vessel along its trajectory, accounting for increased noise while fishing, generate noise maps for a specific area and time period, or create time-lapse videos illustrating underwater noise dynamics.

A further proposal in this setting that demonstrates the potential of using AIS data for underwater noise estimation is Jallkanen et al. in [29]. This work uses worldwide terrestrial and satellite AIS data covering the years 2014-2020 and the STEAM (Ship Traffic Emission Abatement Model) tool by the Finnish Meteorological Institute [30] to estimate vessel noise

Table 1 No. of vessels, AIS records, and trips for the year 2020, April, and June 2020

Period	No. Vessels	No. AIS records	No. Trips
Year 2020	714	92, 916, 965	72, 776
April 2020	548	5, 392, 677	4, 923
June 2020	642	9, 841, 079	7, 462

source levels. The STEAM model predicts instantaneous vessel noise levels that were then cumulated over time to produce a noise source energy map. The instantaneous noise levels in each vessel position (and in a sphere around the source) were reported in a spatiotemporal grid cell, whose resolution is 0.1^{o} (WGS84 coordinate system). The gridded data were produced for the frequencies 63 Hz, 125 Hz and 2000 Hz. Results included a quantification of the global underwater noise emissions from shipping in the period 2014-2020 (showing that at the current rate the emissions are doubling every 11.5 years), a study of the emissions in different areas (showing a large variability of shipping noise in different regions), a study on the emissions during the COVID-19 pandemic (showing a drastic reduction of emission levels globally) and a study of the emissions of the various vessels categories (indicating that container ships are the largest contributor to shipping noise emissions).

3 Data sources

In this section, we present the data sources used in this study. Specifically, four datasets are employed: AIS data, information on vessel characteristics, environmental data, and hydrophone data from the SOUNDSCAPE project.

Automatic Identification System (AIS) The Automatic Identification System (AIS) was originally developed as a tool to enhance navigation safety by helping to prevent collisions between vessels as it allows their detection. The *International Maritime Organization*[1] (IMO) requires AIS transmission for ships with a gross tonnage of 300 tons or more, all passenger vessels, and any boat exceeding 15 metres in length. Specifically, AIS data include several key components: the vessel's name; the Maritime Mobile Service Identity (MMSI), which uniquely identifies the vessel; its International Maritime Organization (IMO) number; the vessel's call sign; its position, given by latitude and longitude coordinates (in decimal degrees); the timestamp of the transmission (in UTC); speed over ground (SOG); course over ground (COG); heading; length overall (LOA); and the vessel type (e.g., cargo, sailing boat, fishing vessel). In some cases, AIS data may also provide details such as the starting port, destination, and estimated time of arrival.

We work on a dataset provided by the Italian Coast Guard, consisting of terrestrial AIS data for trawl fishing vessels operating in the Northern Adriatic Sea from January 2020 to December 2020. We remark that this dataset is not public and, currently, we do not have access to AIS data from other types of vessels. It is important to note that the year 2020 represents a period of restricted shipping activity due to the COVID-19 pandemic outbreak. In Italy, a lockdown was imposed from March 9, 2020, until May 18, 2020, during which many activities, including restaurants, were either closed or had to limit their operations. In this study, we focus on April and June 2020, to investigate the differences in environmental pollution during a period when all activities were significantly reduced, compared to a period of regular maritime operations. Table 1 reports the number of vessels, AIS data records, and trips for the year 2020, as well as for April and June 2020.

[1] https://www.imo.org/

Vessel Information In addition to AIS data, knowing the characteristics of the vessels is crucial. Specifically, the Italian Coast Guard provided us with a dataset containing several attributes related to the fishing vessels, including the MMSI of the vessel, the vessel's name, its country, the name of the port where the vessel is registered, the type of gear used, and the engine power (in horsepower). The engine power is particularly important for this study, as it is used to estimate the underwater noise generated by the vessel, as detailed in Section 4.2.

Environmental Data To calculate the propagation of underwater sound, it is essential to consider the environmental factors that play a crucial role in sound absorption. Therefore, we consider daily measurements of sea surface temperature (in degrees Celsius), daily measurements of sea salinity (in PSU, Practical Salinity Units), seawater potential of hydrogen (pH), and sea depth (in metres). The temperature dataset includes 2754 daily measurements, while the salinity and pH datasets each contain 3469 daily measurements. Temperature, salinity, and pH data are sourced from *Copernicus*,[2] whereas sea depth information, consisting of 48826 records, comes from the *European Marine Observation and Data Network* (EMODnet).[3] These environmental features are used to calculate the absorption of sound in seawater (denoted as α) detailed in Section 4.3.

Hydrophone Data To determine the acoustic characteristics of the vessels' engines and fine tune the propagation model, we leverage direct acoustic measurements from the Interreg Project SOUNDSCAPE [13, 21]. The SOUNDSCAPE dataset is composed of 20 and 60 seconds averaged sound pressure levels (SPLs, dB ref 1μPa), recorded across a wide frequency range divided into third-octave bands. These data were collected at nine monitoring stations from March 2020 to June 2021, including the first full lockdown period related to the COVID-19 pandemic (March-May 2020). Figure 1 illustrates the positions and names of the nine monitoring stations set up by the project SOUNDSCAPE.

In this work, we use the 60-second interval dataset and focus on the 63 Hz and 125 Hz frequencies, which are considered standard by the *European Marine Strategy Framework Directive* (MSFD), as well as on 400 Hz and 4000 Hz, due to the increased significance of environmental factors at higher ranges. Higher frequencies are particularly relevant for communication between dolphins.

Table 2 presents, for each hydrophone, its location (latitude and longitude) and the number of records in the dataset of 60-second averaged SPLs (one-third octave, base 10), covering the period from March to December 2020, as well as the months of April and June 2020.

4 Underwater noise model

In this section we describe a model for underwater sound propagation that is used in Section 5 to provide a spatiotemporal characterisation of underwater noise in the Northern Adriatic Sea. We present the theoretical laws governing underwater sound propagation, and we also describe how we obtain the estimation for source sound levels, propagation loss and ambient noise, necessary for the definition of the model. We recall that the estimation is based on the 60-second averaged SPL dataset released by the project SOUNDSCAPE and we focus on the frequencies of 63 Hz, 125 Hz, 400 Hz and 4000 Hz, as explained in Section 3.

[2] https://www.copernicus.eu/en

[3] https://emodnet.ec.europa.eu/en

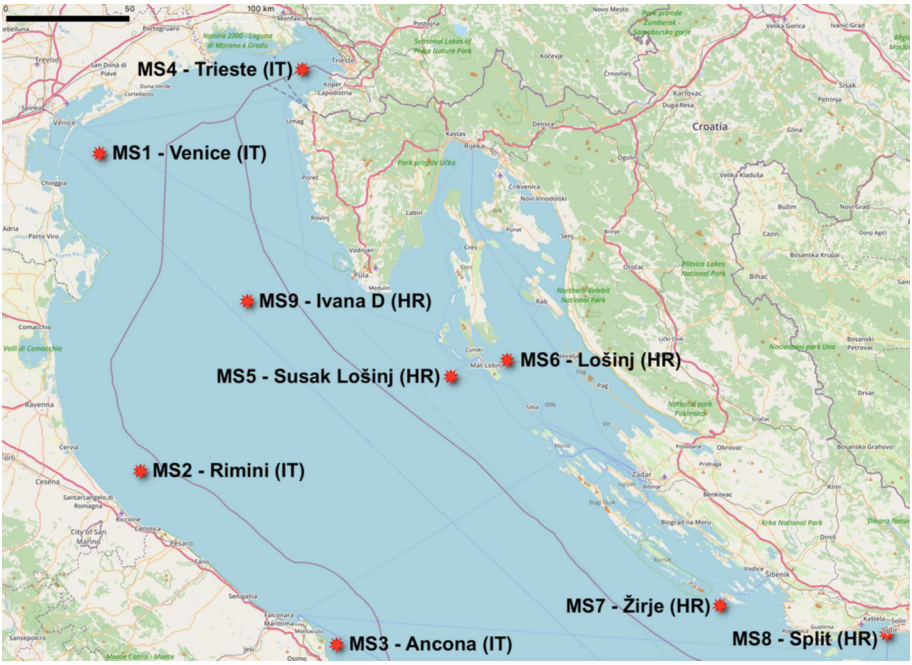

Fig. 1 SOUNDSCAPE hydrophones in the Northern Adriatic Sea

4.1 Sound propagation model

The basic objective of noise modelling is to assess how much noise a particular activity will generate in the surrounding area [31]: the aim is to model the received noise level (RL) at a given point (or points), based on the sound source level (SL) of the noise source, and the amount of sound energy which is lost as the sound wave propagates from the source to the receiver (transmission loss or propagation loss, TL). The relation between these quantities is encapsulated in the classic sonar equation [32]:

$$RL = SL - TL \tag{1}$$

Table 2 Location and number of records for each hydrophone in the 60-second averaged SPL dataset from the SOUNDSCAPE project (March-December 2020, April 2020 and June 2020)

Monitoring station	Longitude	Latitude	Mar-Dec 2020	April 2020	June 2020
MS1 - Venice (IT)	12°30.883′	45°19.383′	387, 432	30, 660	36, 237
MS2 - Rimini (IT)	12°42.656′	44°10.254′	340, 928	43, 200	43, 200
MS3 - Ancona (IT)	13°40.932′	43°31.954′	343, 479	31, 663	29, 767
MS4 - Trieste (IT)	13°33.917′	45°37.095′	318, 533	43, 078	43, 032
MS5 - Susak Lošinj (HR)	14°17.293′	44°29.545′	418, 330	39, 615	39, 173
MS6 - Lošinj (HR)	14°34.510′	44°32.747′	387, 488	12, 126	38, 955
MS7 - Žirje (HR)	15°36.020′	43°37.788′	339, 706	-	43, 200
MS8 - Split (HR)	16°25.336′	43°29.895′	358, 889	43, 200	43, 141
MS9 - Ivana D (HR)	13°15.720′	44°46.953′	217, 928	43, 141	43, 141

This straightforward expression is fundamental to modelling underwater noise, and its simplicity belies considerable complexity in the task of computing the transmission loss in order to estimate the received noise.

Sound propagation is profoundly affected by some factors such as the conditions of the surface and bottom boundaries of the sea as well as by the variation of sound speed within the ocean volume [33]. Air has a density 800 times lower than the density of water, therefore a sound that propagates inside the water has a higher propagation speed, equal to about 1500 m/s, against about 340 m/s of air. So, with a sampling period of 60 seconds it makes sense to neglect propagation time within the area affected by a sound source (area of influence) and, within the sampling interval, consider the noise level distribution as stationary. When a boat switches the engine on, we consider the noise as instantaneously propagated in the area of influence within the sampling period, without actually propagating the wavefront in space-time.

Sound propagation speed is also influenced by various chemical-physical factors such as temperature, salinity and pressure [34], varying both during the day and with the seasons in the superficial part [35], and with depth. In shallow water, that is the predominant context in Northern Adriatic Sea, sound wave reflections off the seabed strongly affect propagation, and bathymetry plays an important role in determining propagation loss [16]. The computation of the transmission loss considering all these parameters is not a simple task and for this reason various models have been introduced. Before discussing the transmission loss, however, we focus on how to evaluate the source level, that is, in our case, the noise generated by the fishing vessels.

4.2 Source level estimation

The principal sources of underwater noise are machinery, propellers, and cavitation. Our AIS dataset and the vessel information dataset contain details about fishing boats, including length overall (LOA), engine horsepower, and fishing gear. However, these datasets do not include direct measurements of the sound pressure levels of the fishing vessels. So, we need to infer such values considering the general literature about underwater noise and the measurements provided by the SOUNDSCAPE project.

A first issue is how to evaluate the increase of noise when a trawler is in action. Many studies focus on assessing the noise of vessels when they are free-running (i.e., when they are not performing fishing activities). However, trawling vessels typically generate higher levels of radiated noise compared to free-running vessels operating under the same machinery settings [36]. While published data on the radiated noise from operating trawling vessels are limited, some studies have reported increases in radiated noise ranging from 5 dB to 15 dB during trawling activities [37]. Specifically, in [36] it is noted that the effect of trawling is minimal below 100 Hz and increases with frequency. Accordingly, we assign an increase of 5 dB at 63 Hz when the vessel is trawling, 10 dB at 125 Hz, and 15 dB at higher frequencies, specifically at 400 Hz and 4000 Hz. This approach aligns with the findings in [37] and reflects the change in source levels during trawling as discussed in [5].

To recover the sound pressure level of a specific fishing vessel, we consider the measurements of the hydrophone MS9 located at $13°15.720E$ $44°46.953N$, in the middle of Adriatic Sea (see Table 2), with 42m-depth, terrigenous sandy seafloor, taken on March 31, 2021 between 5:40 pm and 5:55 pm. Here, there is a unique fishing vessel crossing nearby the hydrophone and taken as the reference boat. Thus, the recorded noise is associated to the trip 1001 of the reference boat (length=27.45 m, engine power=835 Hp), while trawling at about 3.9 kn (knots) between 500 m and 60 m from the hydrophone. A linear regression

was performed between the measured values of SPL, expressed in decibel, and logarithmic distance, thus allowing to assign a vessel with an 835 Hp engine, when not trawling, an estimated source level (at the conventional distance of 1 m from the point source) that varies with frequency as reported in Table 3.

In order to associate the source levels to all the other vessels, we need to relate the sound pressure level to the engine horsepower, the latter being available in our dataset. If we assume that a constant fraction of engine power gets converted into acoustic power (i.e. acoustic power scales linearly with horsepower), then 3 dB are added per doubling in engine power. We adopt such a linear progression on logarithmic scale of engine power and the resulting value is denoted with SL_0. For example, for engines between 100 Hp and 835 Hp, considering a frequency of 63 Hz, we obtain a range between 123 dB and 136 dB.

Differences in source level may result from variations in speed. Specifically, as noted in [15], the intrinsic factor of speed can influence the broadband source level of ships according to the following relation:

$$SL = \begin{cases} SL_0 & \text{if } v \leq v_0 \\ SL_0 + 15.39\, dB \times log_{10} \frac{v}{v_0} & \text{if } v > v_0 \end{cases} \tag{2}$$

where $v_0 = 3.9$ kn corresponds to the speed of the reference boat and v is the actual speed of the vessel. For simplicity, we assume that our model source boat radiates uniformly in all directions, although the acoustic signature of actual boats in navigation is louder from the side-aspect and stern-aspect than from the bow-aspect.

4.3 Transmission loss

In the ideal scenario, where surface and seabed reflections as well as absorption losses are neglected, and propagation speed is uniform, simple spherical spreading governs transmission loss [38]:

$$TL = 20 \times log_{10}(r) \tag{3}$$

where r is the distance between the source and the receiver.

As observed in more realistic scenarios, sound will initially exhibit spherical spreading at short distances, where boundary effects are negligible, followed by cylindrical spreading at long ranges. In between, there is a transition region where neither spherical nor cylindrical spreading accurately describes the sound propagation. This situation can be approximated by assuming a sudden shift from spherical to cylindrical spreading at a *transition range* r_{trans}. While some recommend using the water depth as a rough estimate for this transition range, it is important to use this approach with caution. As highlighted in [38], the optimal transition range r_{trans} varies depending on seabed characteristics. Simulation by parabolic equation modelling [39] (confirmed by normal-mode modelling) shows that for a flat bottom at 50 m-depth (soft seabed, $\rho = 1500$ kg/m^3, $c = 1700$ m/s), there is about 48 dB attenuation at 400 m, corresponding to over 8 doublings with spherical attenuation. Between 2 and 4 km the attenuation is about 4.5 dB, which is compatible with mode stripping attenuation (between

Table 3 SPL for the reference boat at different frequencies

	63 Hz	125 Hz	400 Hz	4000 Hz
SPL (1m)	136 dB	133 dB	126 dB	123 dB

spherical and cylindrical): 15 $log_{10}(r)$. Propagation modelling and experimental measurements in [40] show decreased attenuation in shallow water. For soft seabeds, propagation loss is greater than for hard seabeds, but attenuation is lower at 15 m than at 30 m depth. Up to 100 m, at 30 m-depth, with soft seabed, sound pressure decrease is almost identical to spherical spreading. At 15 m-depth, with soft seabed, sound pressure decrease is spherical up to about 60 m, then the decrease is much lower. The same study reports a 4 dB increase in sound level when speed changes from 6 to 11 kn, confirming the velocity-dependent component of 15.39 dB $\times\ log_{10}\frac{v}{v_0}$ from (2). In [16] Ainslie proposes a modification to cylindrical spreading for long ranges, once the reflection losses due to multiple bottom reflections begin to accumulate. Following [16], we adjust the propagation loss to implement the combination between spherical propagation and mode stripping as follows:

$$TL = \begin{cases} 20\ log_{10}(r) & \text{if } r \leq r_{trans} \\ 15\ log_{10}(r) + 5\ log_{10}(r_{trans}) & \text{if } r > r_{trans} \end{cases} \tag{4}$$

The 15 $log_{10}(r)$ dependence on range is known as mode stripping because it results from the gradual erosion of steep ray paths (high-order modes) after multiple bottom reflections. To determine r_{trans}, we refer to the trajectory of trip 1001 of the reference boat. At 63 Hz the transition is expected to occur at around 400 m, approximately 10 times the water depth. This indicates that r_{trans} is parametrically dependent on depth through a multiplicative factor of 10. For the middle frequencies (125 Hz and 400 Hz) we set the commutation between the two propagation regimes at 4 times the depth based on our simulations. For the highest frequency (4000 Hz) we restrict such commutation range even further, to twice the depth.

With simple geometric spreading, the role of absorption in propagation is not accounted for. Environmental absorption features may affect the transmission loss, especially for large distances and high frequencies. In more realistic models, one needs to consider all the environmental aspects that influence the sound propagation underwater, by adding a term proportional to distance from the source [38]:

$$TL_{tot} = TL + \alpha \times r \tag{5}$$

In the literature there are several models for predicting the absorption of sound in sea water which retain the essential dependence on temperature, pressure, salinity, acidity and other environmental features. In the Francois and Garrison model [41] the general equation for the absorption of sound in sea water, at a given frequency f, is given as the sum of contributions from boric acid, magnesium sulfate, and pure water. At a frequency below 100 Hz only the first contribution is relevant, as α is approximately of the order of 10^{-6} dB/m [38]. Specifically, at frequencies of 63 Hz and 125 Hz, α is on the order of 10^{-6} dB/m, while at 400 Hz it increases to the order of 10^{-5} dB/m, and at 4000 Hz it reaches the order of 10^{-4} dB/m.

4.4 Ambient noise

The received noise level (RL) at a given point is computed starting from (1). However, the formula does not consider the ambient (or background) noise, which is present in the marine environment. The received noise level RL exceeding ambient noise is

$$RL = SL - TL_{tot} - AN \tag{6}$$

where SL is the sound source level, TL_{tot} the transmission loss and AN the ambient noise.

We use the SOUNDSCAPE measurements also to estimate the ambient noise. In particular, we employed the exceedance level L_{90} [17], which indicates the sound level that is exceeded 90% of the time and is equal to the 10^{th} percentile statistic. As mentioned in [18], L_{90} can be referred to the common natural acoustic conditions. This sound level is very different at the nine stations along the year and at the various frequencies (see Fig. 3 in [18]). Hence, for each frequency and for each month of the year, we compute the *ambient noise map* in the following way. We partition the Northern Adriatic Sea into a regular grid composed of square spatial cells (1km×1km). The cell size was defined by environmental experts to ensure an adequate representation of sound propagation while maintaining a balance between computational efficiency and spatial accuracy. Given a certain frequency and a month, to assign an ambient noise value to each cell of our grid, we started from the cells where hydrophones are located: we associated the exceedance level L_{90} of the hydrophone at the corresponding cell. Then we applied an Inverse Distance Weighting (IDW) interpolation using QGIS,[4] an Open Source GIS that supports viewing, editing, and analysis of geospatial data. In this type of interpolation, the sample points are weighted so that the influence of each point decreases with distance from the unknown point being estimated. This approach allows us to assign an ambient noise value that varies for each grid cell, capturing the differences in underwater noise across various regions of the Northern Adriatic Sea. For instance, in June 2020, at 63 Hz the most silent area is Ancona (Italy) with an ambient noise of 60.78 dB and the loudest zone is Žirje (Croatia) with a value of 82.62 dB. Instead, at 4000 Hz Ancona has an ambient noise of 84.65 dB and Žirje reaches a value of 92.80 dB.

4.5 Aggregating received noise levels

At a measurement point that is equally distant from two equally-powerful sound sources, the two contributions would add up in magnitude and phase. However, distinct and independent sources, such as two boats, can be treated as incoherent sources. Even in a narrow frequency band, there will be a random phase difference between the two sources. Therefore, the noise in a 1/3 octave band around 63 Hz (or in any other band) gets increased by 3 dB if there are two equal contributions, by 6 dB if there are four equal contributions, etc. [20]. More precisely, what is added are the intensities, after inversion of the logarithmic function that defines the decibel. Generally, if we have n sources reaching a cell with n different values of RL, the total noise level is:

$$RL_{total} = 10 \times log_{10}(10^{RL_1/10} + \ldots + 10^{RL_n/10}) \tag{7}$$

5 Implementation using MobilityDB

In this section we develop a framework for the spatiotemporal characterisation of underwater noise. As already mentioned, we partition the Northern Adriatic Sea into a regular grid composed of square spatial cells (1km×1km) and we estimate the noise generated by the fishing vessels in any cell at regular time intervals (every 60 seconds). We retain the 60-second interval temporal resolution to be synchronised with the SOUNDSCAPE project's measurements. The overall process is illustrated in Fig. 2. Starting from AIS data, vessel information, and hydrophone data, we estimate the source level produced by the vessels. We then incorporate environmental factors and hydrophone data to enrich the grid of the Northern

[4] https://qgis.org/en/site/

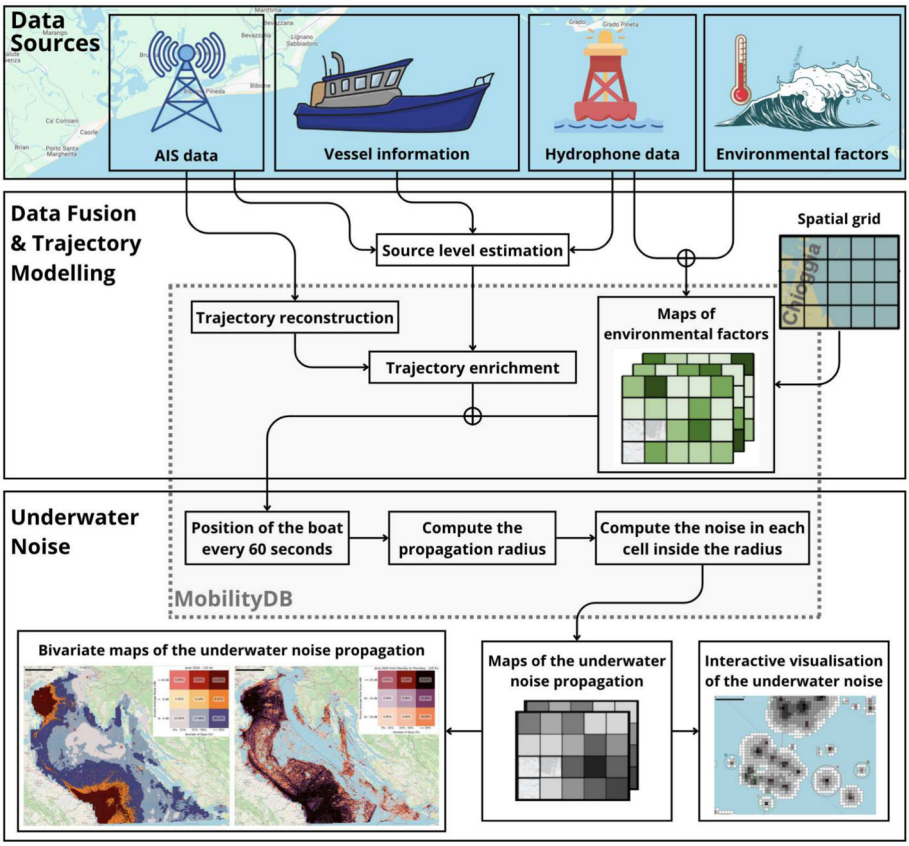

Fig. 2 Overview of the process consisting of three main steps: data sources, reconstruction and enrichment of trajectories, and underwater noise propagation

Adriatic Sea with environmental variables such as sea salinity, sea surface temperature, sea depth, pH, and ambient noise. Using AIS data, we reconstruct vessel trajectories and further enhance them with semantic information, building on our previous work [10, 11], as detailed in Section 5.1. Based on these semantic trajectories and the enriched grid, we develop our sound propagation model, which is described in Section 5.2. Finally, we generate underwater noise maps, which are crucial for ecologists and policymakers to study underwater noise pollution and ensure a productive and healthy marine ecosystem. Most of this process (including trajectory reconstruction and enrichment, the development of the spatiotemporal grid, and sound propagation modelling) is implemented using MobilityDB, a moving-object database for managing and analysing trajectories. Further implementation details and the advantages of using MobilityDB are discussed in Section 5.3.

5.1 Creation and enrichment of vessel trajectories

The first step consists in reconstructing the trajectories of the fishing vessels starting from terrestrial Automatic Identification System (AIS) data, i.e., the AIS data sent by ships and received by ground stations on the Italian coast of Northern Adriatic Sea. As described in Section 3, AIS data contains the identifier of the vessel, called MMSI, its position and the

time instant of the bearing, together with other information, like speed and course. Since boat positions are recorded every 10-20 seconds, which correspond to a small spatial displacement of the boat, trajectories are reconstructed by linear interpolation of the AIS data. Next, in order to organise the data into distinct trajectories followed by the fishing vessels, also called trips, the continuous movement of a vessel is split according to several criteria. For example, a new trip begins when the vessel is inside a port area and there is no AIS transmission for longer than a fixed time (see [11] for more details).

A trip consists of a sequence of segments obtained by connecting consecutive AIS points. The next step is to enrich such trajectories with different kinds of semantic information, called *aspects*, following the MASTER model [9]. The model distinguishes among *long-term* aspects (associated with the full trajectory), *volatile* aspects (associated with the segments) and *permanent* aspects (associated with the fishing vessel, derived from the MMSI). A *long-term* aspect is the length and the duration of the trajectory whereas a *permanent* aspect, defined for this specific work, is the sound level associated with the engine horsepower of the vessel, SL_0. This aspect is computed as specified in Section 4.2, and it is denoted by $mmsi.SL_0$. Two crucial *volatile* aspects are the *speed* of the vessel and the *activity* carried out by the fishing vessel. We consider the following activities: *in port*, *entering to* and *exiting from* the port, *navigation* and *fishing*. The *in port*, *entering to* port and *exiting from* port situations can be deduced from the position of the extremes of the segment w.r.t. the port area. If none of the previous cases applies, the *fishing* or *navigation* activities are established on the basis of the average speed of the boat. This aspect is of fundamental importance for the underwater sound propagation model, because when a boat is fishing it produces a much more intense sound. Given a spatiotemporal point $p = ((x, y), t)$ belonging to a segment s ($(x, y) \in s$) in a certain time interval I ($t \in I$), $p.speed$ denotes the speed of the vessel in p, and we set $p.fishing$ to 1 if the activity associated to the segment s during I is *fishing*, 0 otherwise.

5.2 Construction of the noise maps

In this section we describe the high-level procedure for assigning a noise level at a certain frequency f induced by the fishing vessels to the cells of a regular grid, partitioning the Northern Adriatic Sea, every 60 seconds. We consider a set of spatiotemporal cells $\mathbb{G} = \mathbb{S} \times \mathbb{T}$ where $\mathbb{S}$ is a regular grid consisting of 1km$\times$1km spatial cells, and $\mathbb{T}$ is a set of time instants, such that t_0 is a fixed time instant and $t_{i+1} = t_i + 60s$. Hence, each spatiotemporal cell $c \in \mathbb{G}$ consists of two components, (g, t), representing the spatial cell g at time instant t. For each frequency $f \in \{63, 125, 400, 4000\}$ we write $\mathbb{G}_f$ to denote the set of spatiotemporal cells annotated with pieces of information which possibly depend on the chosen frequency. The annotations are: (i) *ctd* contains the coordinates of the centroid of g; (ii) *depth* stores the depth of the sea in c; (iii) α stores the absorption of sound as defined in Section 4.3; (iv) *an* records the ambient noise in c estimated as reported in Section 4.4; (v) *rl* records the total noise received in c, i.e., by the centroid of g at time instant t. It is worth noticing that only the latter three annotations depend on the frequency f.

Let $\mathcal{TR}$ be the set of the trajectories of the fishing vessels, $\mathbb{G}_f$ be the spatiotemporal grid with $f \in \{63, 125, 400, 4000\}$. Algorithm 1 computes the total received noise level for every cell $c \in \mathbb{G}_f$ at the frequency f. We use $p \downarrow 1$ to denote the projection on the first component of the spatiotemporal point p, i.e., its coordinates, and $\mathrm{d}(z_1, z_2)$ for the Euclidean distance between two spatial points z_1 and z_2.

The noise is estimated every 60 seconds at the selected frequency, i.e., in the time instants belonging to $\mathbb{T}$ at frequency f. The centroids of the grid cells are considered as virtual

Algorithm 1 Given $\mathcal{TR}$, $\mathbb{T}$, $\mathbb{G}_f$ and $f \in \{63, 125, 400, 4000\}$, the algorithm computes the total received noise level for each $c \in \mathbb{G}_f$ at frequency f.

```
1: Let mp: map⟨cell, float⟩
2: for each tr ∈ TR do
3:    for each t ∈ T do
4:       p = (tr(t), t)
5:       c_p = unique cell c ∈ G_f such that p ∈ c
6:       v_0 = 3.9
7:       if p.speed > v_0 then
8:          SL = tr.mmsi.SL_0 + 15.39 · log_10 (p.speed / v_0) + inc_f · p.fishing
9:       else
10:         SL = tr.mmsi.SL_0 + inc_f · p.fishing
11:      end if
12:      r_trans = c_p.depth · mult_f
13:      r = 10^((SL − 5·log_10(r_trans) − c_p.an)/15)
14:      for each c = (g, t) ∈ G_f. d(c.ctd, p↓1) < r do
15:         dist = d(c.ctd, p↓1)
16:         if dist ≤ r_trans then
17:            RL = SL − 20 · log_10(dist) − c.α · dist − c.an
18:         else
19:            RL = SL − 15 · log_10(dist) − 5 · log_10(r_trans) − c.α · dist − c.an
20:         end if
21:         mp[c] = mp[c] + 10^(RL/10)
22:      end for
23:   end for
24: end for
25: for each c ∈ G_f do
26:    c.rl = 10 · log_10(mp[c])
27: end for
```

listening points (we have 43, 386 of these points), and consequently the noise *received* at a centroid point models the noise in all the points of the cell at a certain time instant and at frequency f.

In order to build the noise map at frequency f, we get the positions of all the fishing vessels at the same time instants, i.e., every 60 seconds. For each point (Line 4), we determine the cell it belongs to (Line 5) and we calculate the noise generated by the fishing vessel (Lines 7–11) obtained by adding to the sound level associated with the horsepower of the boat ($mmsi.SL_0$), a contribution related to the actual speed of the vessel in p (see (2)), and the noise due to the fishing activity if it occurs in p. Notice that the latter, inc_f, can range from 5 dB up to 15 dB depending on the frequency, as discussed in Section 4.2. In Line 13, the sound propagation radius r (expressed in metres), i.e., the distance at which the noise generated by the fishing vessel gets drowned into ambient noise, is computed. This is obtained by using (6) and setting the received noise (RL) to 0:

$$0 = SL - TL_{tot} - AN$$

In computing the radius we ignore the coefficient of absorption α in (5) for TL_{tot}, allowing for a simplification of calculation and getting an overestimation of r, hence the approximation is safe. With some simple mathematical steps we get $r = 10^{(SL - 5\cdot\log_{10}(r_{trans}) - c_p.an)/15}$ where r_{trans} is the transition range when spherical propagation shifts to a lower attenuation. Its value depends on the sea depth in c_p (Line 12) and it varies according to frequency f, $mult_f$, ranging from 2 up to 10 times the sea depth, as explained in Section 4.3. Then, we propagate the noise in the cells that are within the radius r (Lines 14–21) according to (4) and we

compute the relative received noise level by (6). Finally, by using (7), we combine all the received sound levels to obtain the total noise level at frequency f to be associated with the cell (Line 26).

Concerning the complexity, let $n = |\mathcal{TR}|$, $m = |\mathbb{T}|$, $k = |\mathbb{G}|$, a be the area of a grid cell and r the largest radius arising in Line 13. Then the complexity is $O(n \cdot m \cdot r^2/a + k)$. The factor r^2/a is motivated by the fact that in Line 14 we consider the cells in a neighbourhood of radius r. Note that r depends on the source level, which is bounded by the maximum engine power and the maximum speed of the monitored fishing vessels. In our case, the radius r for each frequency is less than 71,254 m for 63 Hz, 111,399 m for 125 Hz, 31,802 m for 400 Hz, and 5,478 m for 4000 Hz.

In order to process all this data and build our model, we used a machine that features 32 Intel(R) Xeon(R) CPU E5-4610 v2 processors running at 2.30 GHz, offering multithread performance. It is equipped with 256 GB of DDR4 ECC RAM and it utilises a 500 GB RAID 5 storage configuration. On this machine we deployed PostgreSQL 16.6, PostGIS 3.5, and MobilityDB 1.3. Regarding the execution time required to build the sound propagation model from AIS data, it is important to distinguish between the reconstruction and enrichment of vessel trajectories and the propagation of underwater noise. We provide the performance for June 2020, as it is one of the months with the highest number of AIS records. Specifically, the reconstruction and enrichment of fishing vessel trajectories from AIS data for this month take only 46 minutes. The execution time of underwater noise propagation depends on the frequency used, as it varies across frequencies due to differences in ambient noise, vessel SL, the increase in SL during fishing activities, and the absorption coefficient α. For the entire month of June, the execution time required to propagate the underwater noise, starting from the semantically enriched trajectories, is approximately 44 hours for 63 Hz and 125 Hz frequencies, 10 hours for 400 Hz, and 1 hour for 4000 Hz.

This paper focuses primarily on assessing the feasibility of the model and demonstrating its potential through various analyses, rather than optimising its efficiency. A more in-depth evaluation of computational performance, including code optimisation and execution time improvements, is addressed in our recent work [42].

5.3 Implementation details

To construct and store the set of trajectories and to implement the underwater noise model, we used MobilityDB [14], a moving-object database that extends the type system of PostgreSQL and PostGIS with abstract data types supporting spatiotemporal types and operators to manage moving objects. The offered constructs perfectly suit the representation of trajectories, which can be reconstructed from a sequence of spatiotemporal data, and allow for semantic enrichment of trajectories. Moreover, it offers spatial and spatiotemporal indices to improve the efficiency of the high-level procedure described in Algorithm 1.

The motivations behind our choice of MobilityDB for implementing Algorithm 1 are as follows. The size of the datasets implies that the processing must be made in a database context. For this reason, we decided to use PostgreSQL and its spatial extension PostGIS. Although PostGIS enables the representation of trajectories, in which the timestamps are encoded in the M dimension, the temporal support provided is rather limited. MobilityDB extends PostgreSQL and PostGIS with temporal capabilities and provides a rich API for manipulating temporal types. This enables to express processing pipelines such as the one depicted in Algorithm 1 using PL/pgSQL, PostgreSQL procedural language, which adds control structures to the SQL language to perform complex computations.

MobilityDB is implemented in C, as it is PostgreSQL and PostGIS. PostgreSQL takes care of the store and management of the tables as well as bringing the data from disk storage to main memory, where the processing is performed. As the query results are represented as tables, the user may decide to store them back to the database for further processing.

Regarding performance, MobilityDB has efficient data structures that are optimised for temporal data management. Over these structures, a rich temporal algebra and specialised spatiotemporal indices are defined. In addition, the MobilityDB data model enables a *lossless* data compression by removing redundant measures when the value does not change or when it can be derived from other values with linear interpolation. This process, called *normalisation*, enables high compression rates on real-world data, which also enhances the performance.

Finally, expressing spatiotemporal processing in a high-level language such as SQL has multiple advantages. These include, from the user perspective, a better abstraction level for formulating complex spatiotemporal pipelines such as those implemented in Algorithm 1, and from the implementation perspective, that the database management system can perform efficient query processing estimating the best execution plan for the SQL queries.

Let us present the structure of the table storing the trips of the fishing vessels:

```
CREATE TABLE vessel_trip (
      index integer PRIMARY KEY GENERATED ALWAYS AS IDENTITY,
      trip_id integer,
      mmsi integer NOT NULL,
      vessel_name character varying,
      speed tfloat,
      activity tint,
      trip tgeompoint,
      traj geometry
);
```

Each trip is identified by the attribute `trip_id` and it is related to the fishing vessel having `mmsi` and `vessel_name`. The attributes `speed` and `activity` model the *volatile* aspects representing the speed and the activity of the vessel during the voyage and the attribute `trip` models the spatial coordinates of the movement followed by the vessel. These three attributes have temporal types, allowing for the representation of the variation in time of the speed, the activity and the position of the fishing vessel starting from the AIS data. The values between successive instants are interpolated using a linear function for `speed` and `trip` whereas for `activity` a step function is used. Finally, the attribute `traj` with type `geometry` is employed to visualise the trajectory.

To improve the spatial operations on trajectories, like `ST_Intersects`, we add a spatial index on the attribute `traj` of the table `vessel_trip`:

```
CREATE INDEX Vessel_Trip_Geom_Idx ON vessel_trip USING gist(traj);
```

Indexing speeds up searching by organising the data into a search tree which can be quickly traversed to find a particular record. The spatial index structure used is *R-Tree*.

Once reconstructed the trajectories from the AIS data, we need to get the values of all the trajectories at the same time instants, every 60 seconds. MobilityDB offers an efficient function, `tsample()`, to sample a temporal value according to period buckets. We apply such a function to get speed, activity and position every minute, i.e., `tsample(speed,'1 min')`, `tsample(activity,'1 min')`, `tsample(trip,'1 min')`, and these values are inserted into the table `vessel_trip` for the attributes `speed`, `activity` and `trip`, respectively. In this way the three temporal values are built on the same set of minutes, which is $\mathbb{T}$. Figure 3 displays an example of the values for the attributes `activity`,

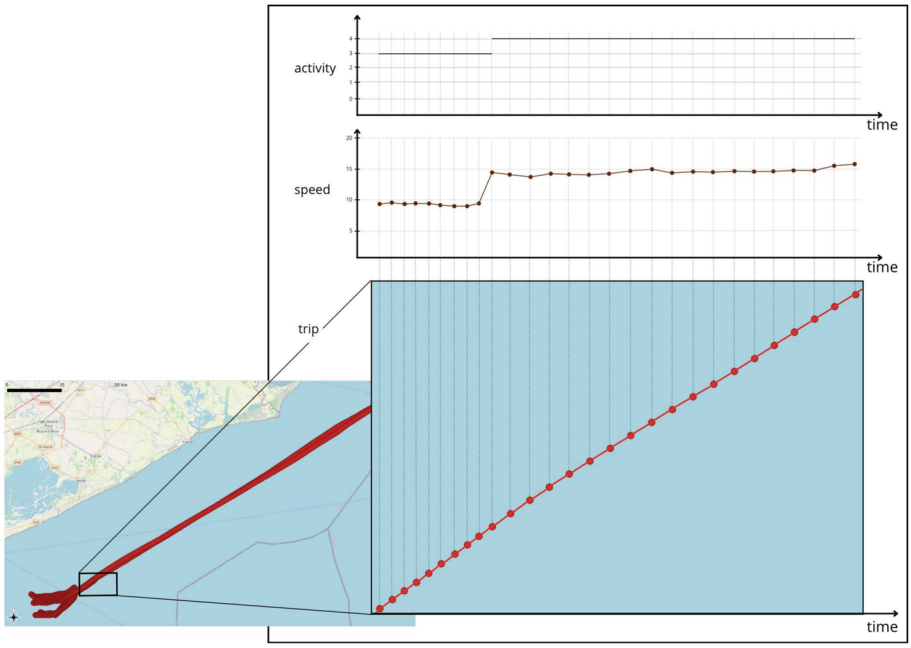

Fig. 3 Representation of the three temporal types `activity`, `speed` and `trip`

`speed` and `trip`. The vertical lines represent the time instants, the three attributes are synchronised and the sample period is one minute. `Trip` represents the movement of the fishing vessel, which consists of a sequence of points whose distance between consecutive points becomes larger because the speed increases. In fact the temporal value `speed` shows a variation from 10 kn up to 15 kn. This change of speed causes a shift in activity as well: the attribute `activity` varies from 3 denoting *fishing* to value 4 indicating *navigation*.

In order to compute the total received noise level for each cell of our grid at a given frequency f, we proceed as specified by Algorithm 1 and illustrated in Fig. 4. For each spatiotemporal point p belonging to `trip` we compute the propagation radius r. By using

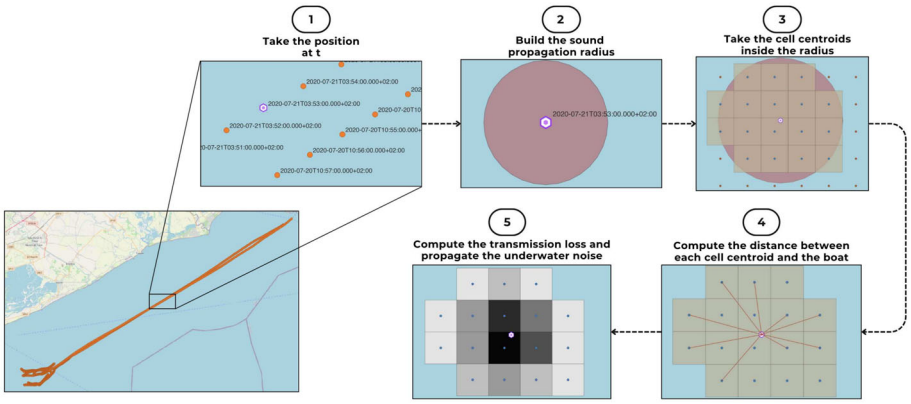

Fig. 4 Main steps in the calculation of the noise maps

the function `ST_Buffer` we build, around the spatial coordinates of p, a buffer b with radius r (Step 2 in Fig. 4). Then, we select all the cells whose centroids are inside b through the predicate `ST_Intersects` (Step 3 in Fig. 4) and we compute the distance between the point p and these centroids (Step 4 in Fig. 4). We use this distance to estimate the transmission loss which allows us to determine the received noise level in the selected cells. By grouping by cell id and time, we combine all the contributions of the points of the different trajectories through (7) (Step 5 in Fig. 4).

6 Analyses and results

In this section we present some analyses performed by using our spatiotemporal characterisation of the underwater noise. We also outline some considerations on model validation, discussing how our model can be compared with the spatiotemporal characterisation provided by the SOUNDSCAPE project.

6.1 Impact of fishery on underwater noise: experimental results

In the following, we illustrate the results of some experiments, which aim at estimating the impact of fishing activities on underwater noise while also demonstrating the expressiveness and flexibility of our approach.

6.1.1 Underwater noise maps at different frequencies

The first experiment consists of assessing the impact of the fishing activity on the underwater noise level considered at different frequencies. Our framework allows us to perform this analysis according to various time granularities, e.g., yearly, seasonally, monthly or daily. We chose to focus on June 2020 because it is one of the months with the highest fishing activity in that year. For this period, the AIS dataset consists of 9, 841, 079 records, belonging to 642 fishing vessels (see Table 1).

As explained in Section 3, we consider the frequencies of 63 Hz, 125 Hz, 400 Hz, and 4000 Hz. For each frequency, we created a bivariate map for June, illustrating two variables at once. The first variable represents the average underwater noise that exceeds the ambient noise, while the second indicates the percentage of days in the period of analysis (1 month) in which a cell is active. For a cell c, a day d is called *active* if the received sound level on d in c exceeds the ambient noise. Bivariate maps are crucial for understanding underwater pollution, as the damage on living species depends both on noise level and noise persistence. Elevated noise levels over a short duration do not affect marine life as significantly as noise at prolonged intervals, which can have more severe consequences for aquatic ecosystems.

In Fig. 5, we can observe the bivariate maps for June for the frequencies of 63 Hz, 125 Hz, 400 Hz, and 4000 Hz. This figure clearly demonstrates that the impact of fishing vessels varies significantly depending on the frequency analysed. These variations stem from several frequency-dependent factors: the initial SPL (SL_0), the absorption coefficient (α), the increased noise generated by the vessel during fishing activities, and the ambient noise, which rises with higher frequencies. For example, at 63 Hz, ambient noise starts at 60.78 dB, whereas the lowest value at 4000 Hz is 81.07 dB. Figure 5d shows that at 4000 Hz, fishing vessels have a negligible impact on the underwater environment: all the cells are characterised by excess noise levels below 4 dB and only 4% of the study area exhibits persistence greater than 50%, i.e., two weeks (dark blue cells). In the majority of the cells, 76%, the excess noise has a low persistence, below one week (light pink cells). Figure 5c displays that at 400 Hz

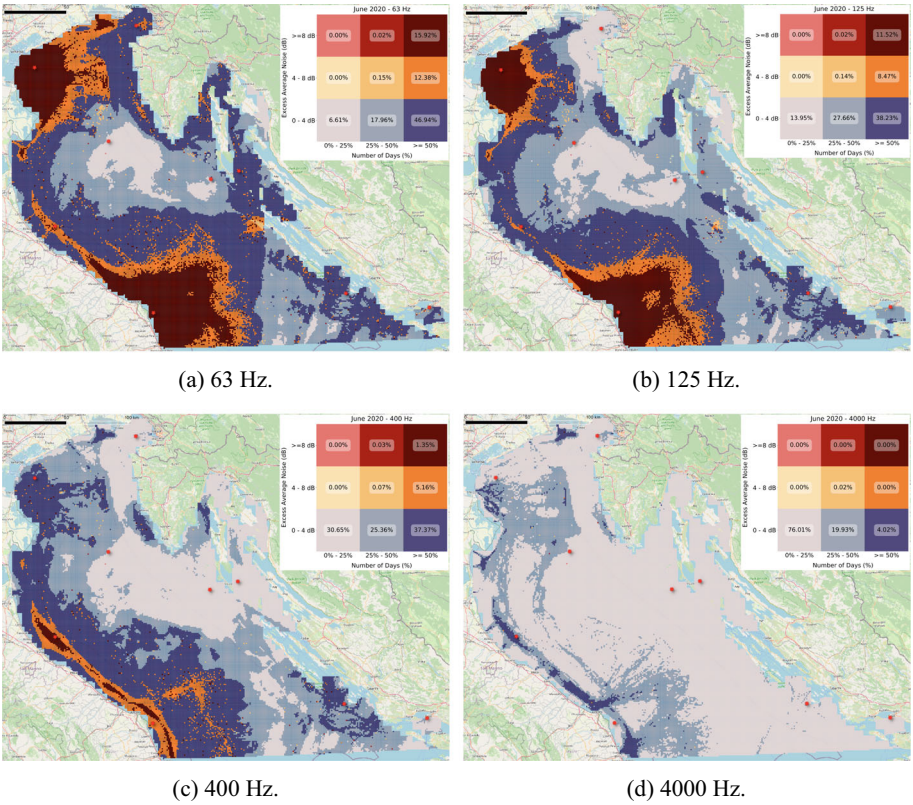

(a) 63 Hz. (b) 125 Hz.

(c) 400 Hz. (d) 4000 Hz.

Fig. 5 Underwater noise bivariate maps for June 2020. The red stars are the hydrophones of SOUNDSCAPE

still 93% of the basin presents excess noise level below 4 dB but now there is an area along the Italian coast, including several harbours, like Rimini and Ancona, extending southward to Civitanova Marche (which marks the southernmost boundary of the map) where the excess noise level is between 4 dB and 8 dB for a persistent period (more than 50% of the days - dark orange cells) reaching the peak over 8 dB in a very limited zone (only 1.35%). Besides, the area with low excess noise level and low persistence, depicted in light pink, is less than half (around 31%) of that obtained for the frequency 4000 Hz.

Figure 5a and b illustrate that at 63 Hz and 125 Hz, fishing vessels have a significant impact on the ecosystem. In fact, more than 20% of the basin, in areas of the Northern Adriatic Sea that are most frequently used for fishing, such as in front of Venice and near Ancona and along the Italian coast, the excess noise levels are over 4 dB with large persistence (more than two weeks – dark orange and dark red cells). At 63 Hz there is the highest percentage of cells (almost 16%) with the highest excess noise levels (greater than 8 dB) for a long time (over two weeks – dark red cells) and the lowest percentage (6.6%) of cells with excess noise levels under 4 dB for less than 1 week (light pink cells).

6.1.2 Effect of the COVID-19 pandemic

In order to investigate the effect of the COVID-19 pandemic outbreak on underwater noise due to fishing activities in the Northern Adriatic Sea, we focus on April and June 2020.

While April 2020 is a month during the lockdown, June 2020 represents the post-lockdown period, during which fishing activities gradually returned to pre-pandemic levels, reflecting the easing of restrictions and a progressive resumption of usual activities. Looking at Table 1, we observe that the number of AIS data in April is limited: only 5, 392, 677 records, slightly more than half of the AIS data in June, despite April typically being a period of intense fishing activity. To compare the during-, and post-lockdown periods, we generated two bivariate maps representing the average underwater noise at 125 Hz that exceeds the ambient noise, along with the persistence of this noise (i.e., the percentage of active days for each cell w.r.t. the total days of the month). Figure 6a illustrates the excess noise map for April, during the lockdown. There is a large portion of the basin, i.e., 82%, with an excess noise level below 4 dB and for 31% of the study area there is also a low persistence (below one week – light pink cells), thus resulting in a very silent sea. The noisiest areas, with excess noise level over 8 dB for a persistent period (more than half a month – dark red cells), are located in the Venice zone, including Chioggia, and from Ancona to the southernmost part of the map. There is also a zone in front of the Croatian coast which shows an increase of noise (excess level between 4 dB and 8 dB and even more 8 dB in several cells) for a persistent period (more than half a month). It is noteworthy that the cells with higher noise levels are located along the coast, and this confirms a redistribution of the fishing grounds, being mainly located near the coasts and in the proximity of the origin harbours as documented in [43]. This behaviour could be due to the possibility to reduce time at sea, limiting the fuel consumption and the related costs. In June (Fig. 6b), there is a significant increase in fishing activities w.r.t. April, as witnessed by the number of AIS data and trips (see Table 1). In the two mentioned zones, near Venice and near Ancona, we observe a boost in the number of cells characterised by elevated noise levels and high persistence (around 3%, dark orange and dark red). Notably, vessels ventured further offshore towards Croatia. Additionally, increased activity is evident in the region near Rimini, indicating greater exploitation of the area. In fact, in June only 14% of the basin is characterised by low noise levels and low persistence (light pink cells). Conversely, cells with noise levels below 4 dB but with persistence greater than 50% (dark blue cells) increase by 12%. These maps clearly points out that the limited fishing activity during the lockdown has caused a reduction in underwater noise, thus proving the acoustic impact of fishery in the Northern Adriatic Sea.

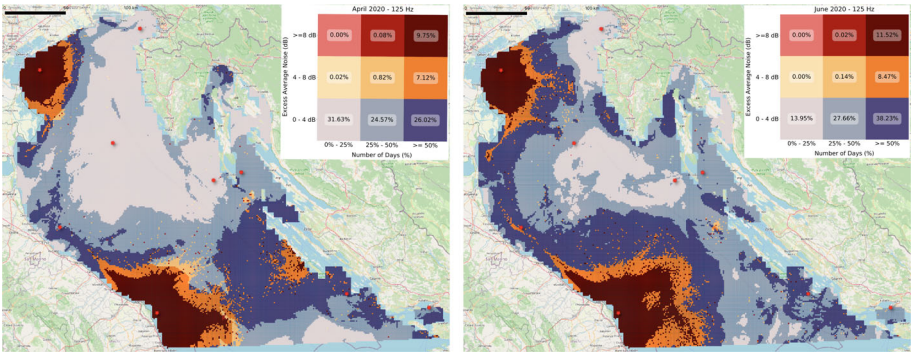

(a) April. (b) June.

Fig. 6 During, and post-Covid underwater noise at 125 Hz for the months of April, and June 2020

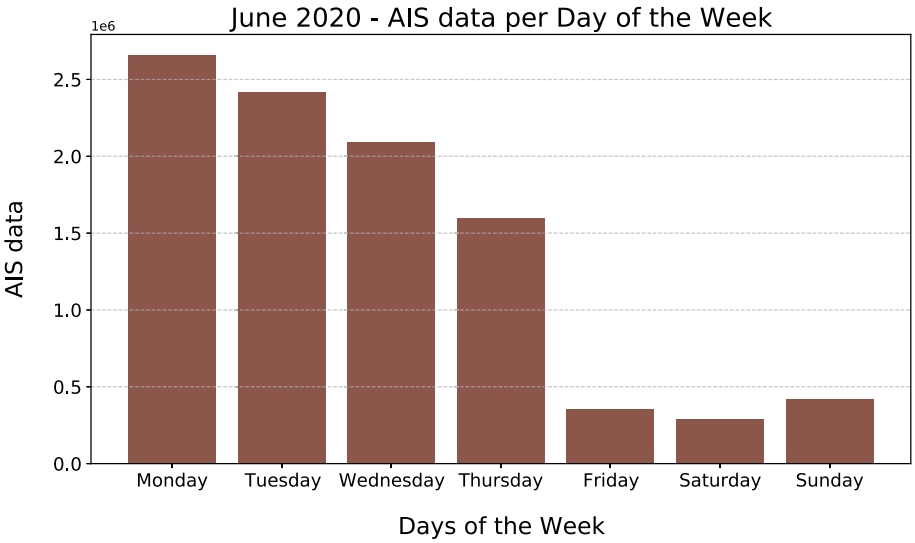

Fig. 7 Number of AIS data per day of the week in June 2020

6.1.3 Focus on the most intense fishing days

In order to deepen the analysis on the areas with the highest noise pressure in the month of June, we investigate how the fishing activity is performed along the days of the week. Figure 7 illustrates the number of AIS data in June 2020 grouped by the day of the week. The plot clearly indicates that fishing vessels concentrate their activity between Monday to Thursday whereas in the weekend a very limited number of vessels go fishing. Hence, we restrict our analysis to the days from Monday to Thursday, using only AIS data within this time frame. The resulting dataset includes 89% of the June data while covering 60% of the days. The possibility to analyse data at different granularity levels is a great advantage offered by our tool.

Figure 8a presents the bivariate map illustrating the average noise that exceeds the ambient noise, along with the percentage of days during the week (from Monday to Thursday) when

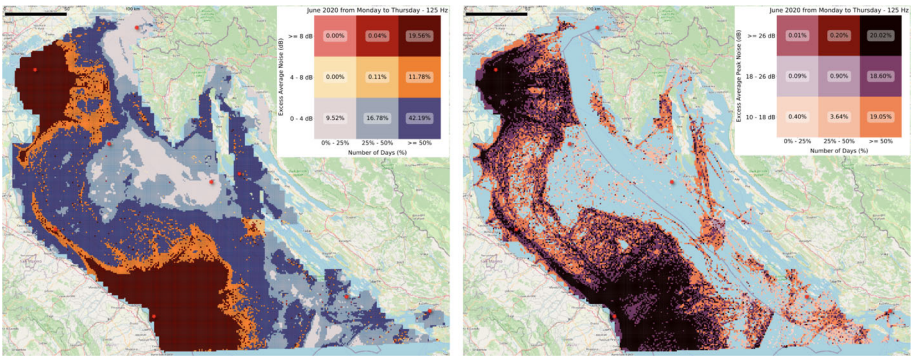

(a) Average underwater noise. (b) Underwater noise peaks.

Fig. 8 Underwater noise in June 2020 at a frequency of 125 Hz from Monday to Thursday

the cells are active. This analysis allows us to highlight the areas swept by fishing vessels during the four days of their highest fishing activity. Notably, we observe an increase in excess noise levels generated during these days and a reduction of the quiet cells. Compared to Fig. 6b, which considers all days of the week, there is a 15% increase in areas where persistence exceeds 50%: the extension of the area with excess noise levels over 8 dB (dark red) is augmented of 8% while the other two areas, i.e, between 4 dB and 8 dB (dark orange) and below 4 dB (dark blue) are enlarged by about 3.5%. On the other hand, the number of cells with excess noise levels below 4 dB and for less than 25% of days decreases by 4.4%. Clearly, the two regions most exploited by fishing vessels - the area in front of Venice and the entire area around and in front of Ancona - remain the same, although with greater noise intensity as well as increased persistence.

To further investigate the noise generated by vessels on these days, we focused on the noise peaks associated with each cell. In particular, Fig. 8b presents a bivariate map where the first variable represents the mean of daily peaks in June 2020 (on a scale starting from 10 dB), while the second variable represents the percentage of active days throughout the month, restricted to Monday through Thursday. Considering the average peaks for the month, the resulting noise is significantly higher; in fact, the bivariate map represents only values exceeding 10 dB. We observe that 19% of the basin includes values between 10 dB and 18 dB, 18.6% are characterised by underwater noise levels between 18 dB and 26 dB, and finally, 20% exhibit noise levels greater or equal than 26 dB, all characterised by a high persistence. Only 37% of the study area has a peak less than 10 dB. This figure clearly points out that the area in proximity of a harbour is noisier and in particular the noisiest zones are located at the south of Venice, in front of Chioggia, as well as the entire zone of Ancona and southward close to Civitanova Marche. Moreover, this map allows us to recover the main routes of the fishing activities.

6.1.4 Interactive visualisation of the underwater noise dynamics

Finally, our implementation provides also the possibility of visualising the spreading of underwater noise in time for a set of vessels. By using *QGIS TimeManager*, it is possible to generate animations which visualise the noise propagation determined by the vessels moving in the Northern Adriatic Sea. The user can choose the boats according to several criteria, such as the range of horsepower, the MMSI, the length overall, or the activity, and the time window of the analysis. In Fig. 9 we can observe a different sound propagation at 125 Hz depending on the engine power of the vessel, its speed and its activity. We focus on four vessels: vessel A has engine power 590.9 Hp, vessel B 613 Hp and vessel C 649.9 Hp (all three with the same SL_0 133 dB), while vessel D has engine power 215.7 Hp (SL_0 130 dB). We can observe that both vessel A and B are fishing (red dot), but vessel A is moving at a speed of 5.67 kn, while vessel B is moving at 2.5 kn. It is worth to remark that the sound propagates across more cells (covering more kilometres) for vessel A compared to vessel B, illustrating how speed affects sound propagation. Vessel C has the same source level as vessels A and B but is not fishing (green dot) and is moving at a speed of 10.75 kn. Compared to vessel A, despite vessel C is moving at a higher speed, the sound propagates less underwater. Specifically, sound propagates approximately 3 km for vessel C and 5 km for vessel A, highlighting the greater impact of fishing activity compared to the vessel's speed. Finally, vessel D has the same speed as vessel C (10.48 kn), and it is not fishing (green dot), but its SL_0 is 3 dB lower. This leads to some differences in sound propagation, as indicated by the reduced number of cells affected by underwater noise for vessel D compared to vessel C, along with the lower noise levels received in those cells. For instance, the cell containing vessel C stores 19.3 dB, whereas

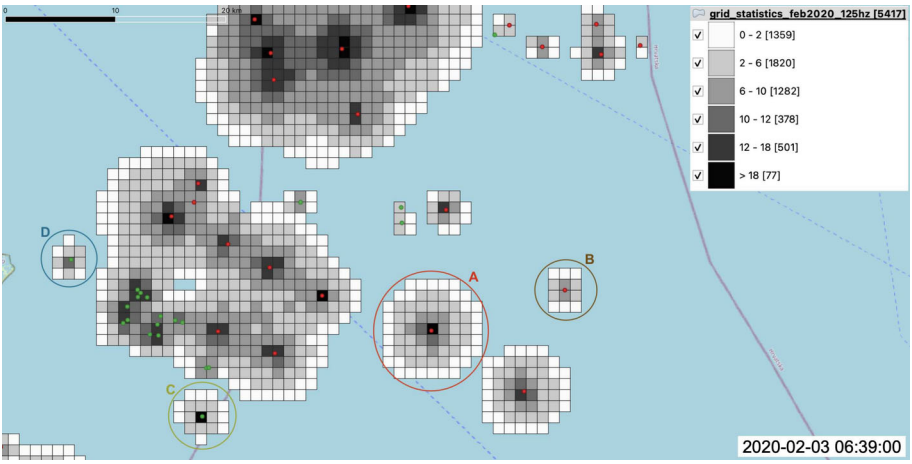

Fig. 9 Propagation of underwater noise of fishing vessels at 125 Hz in the Northern Adriatic Sea on February 3, 2020, at 06:39. Vessels marked with a red dot are fishing, while those marked with a green dot are not fishing

the cell containing vessel *D* records only 11 dB, highlighting a difference of approximately 8 dB. These comparisons show how a fishing vessel generates more substantial underwater noise than a boat merely sailing, even when the latter has a higher speed, as well as how higher vessel speed contributes to greater underwater sound propagation.

Finally, we would like to point out that these are only a few examples of the analyses that can be performed using the spatiotemporal database of semantic trajectories. For instance, we can focus on vessels equipped with specific fishing gear (i.e., LOTB, SOTB, RAP, and PTM) and determine their impact on the underwater noise level. This fine-grained analysis could help to reveal different pollution degrees of fisheries that, in turn, could constitute a basis to implement specific management actions for these activities. Moreover, we can vary our analysis according to different periods and consider only certain sea areas. For instance, one could focus on protected areas, like the Pomo Pit or the Sole Sanctuary.

6.2 Model validation

Our model has been calibrated by using the real measurements provided by the project SOUNDSCAPE. Therefore a natural idea for validating our model might consist in comparing the produced results with the real measurements from the SOUNDSCAPE hydrophones. We start by remarking that a direct quantitative comparison is not possible since our model is aimed to estimate the underwater noise generated only by fishing vessels, while the hydrophones recorded the noise generated by all shipping vessels, including also touristic and commercial vessels. Additionally, the nine monitoring stations are located in fixed positions near ports (except for the MS9 hydrophone, as shown in Fig. 1), where the traffic from other vessel types is certainly present.

Still, some interesting observations can be made, suggesting the adequacy of our model. In general, given that our model restricts to fishing vessels, we can only expect that we provide an underestimation of the underwater noise. An example of proper underestimation is shown in Fig. 10. In light green, the recorded values for hydrophone MS1 clearly detect the passage of a vessel between 5:11 am and 6:12 am, after which the measurements return to the ambient noise level (from 6:13 am to 6:29 am). Instead, our model (dark green) remains constantly

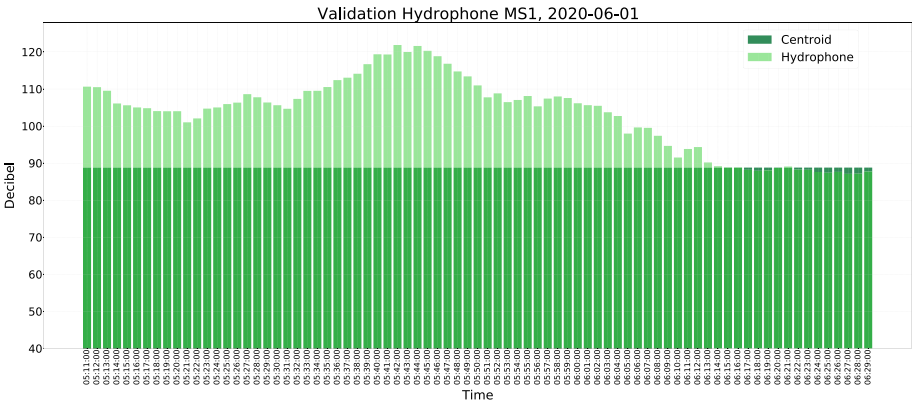

Fig. 10 Underwater noise measurements at 400 Hz from 5:11 am to 6:29 am on June 1, 2020. For each minute, the underwater noise recorded by hydrophone MS1 (in light green) is represented, as well as the noise recorded by the centroid of the cell in which the hydrophone is located calculated using our model (in dark green)

on the ambient noise level. In fact, no fishing vessel passes in the cell where the hydrophone is located during that time period.

A closer correspondence can be detected when a fishing vessel is crossing a cell in which a hydrophone is located. In this case, one can observe a similar trend in the underwater noise level received by the hydrophone compared with the one generated by our model. An example is in Fig. 11a which illustrates minute-by-minute data received by hydrophone MS7 at 125 Hz (in light green) taken on June 22, 2020, from 02:29 am to 02:45 am, compared with the noise levels computed using our model for the virtual listening point located at the centroid of the hydrophone's cell (in dark green). Observe that from 02:29 am the noise level received both at the hydrophone and at the virtual listening point rises, reaching a peak at 02:38 am, before gradually decreasing again until the end of the observations. Some slight differences can be possibly explained by recalling that the centroid and the hydrophone do not share identical geographic coordinates (hydrophone MS7 is situated approximately 274.59 metres away from the cell centroid). Also, variations in environmental conditions and natural sound sources are always present. Figure 11b instead reveals a difference between our noise estimation and the noise measured by the corresponding hydrophone which extends through almost the entire time period of analysis (around one hour). This can be interpreted as a situation in which the hydrophone records the noise produced by a fishing vessel passing through the cell (whose trend is replicated in our model) superposed with additional noise produced by non-fishing vessels that are invisible in our model.

Future improvements in model validation could be achieved by acquiring AIS data for all vessel types, including cargo ships, ferries, and others. This would allow for conducting a well-established procedure for quantitative validation (see e.g. [5, 44]), which is based on the comparison, over a given period, between the hydrophones' measures and the values produced by the model in the nine cells where the hydrophones are placed. However, it is worth noticing that having AIS data from all vessels may not prevent the model from providing an underestimation of the underwater noise, as there are some vessels (e.g. small recreational boats) for which the AIS transceiver is not mandatory.

7 Concluding remarks

Monitoring the underwater noise pollution due to human activities is an important task for maintaining a healthy marine ecosystem. In this paper, we proposed a framework for the characterisation of underwater noise based on semantic trajectories. Starting from the AIS data transmitted by vessels, we reconstructed the vessels' trajectories and deployed them in a spatiotemporal database. The trajectories were enriched with semantic annotations useful to infer how the noise spreads in the area of interest. To estimate the noise generated by vessels, we defined a model for underwater sound propagation based on a combination of spherical and mode stripping propagation. The model takes into account the bathymetry of the area and the relevant environmental variables, such as sea temperature, pH, and sea salinity.

As a case study, we examined the fishing activities in the Northern Adriatic Sea during the year 2020. We implemented the spatiotemporal database of the fishing vessels trajectories using MobilityDB and used it to perform some analyses, aiming to showcase the flexibility and expressiveness of our approach. We presented also a qualitative validation of our model w.r.t. the SOUNDSCAPE measurements. A quantitative validation was not possible because we only consider the AIS data of fishing vessels, so the other marine traffic is invisible to our model. However, for the transits of fishing vessels only, the noise perceived by our virtual listening points seems to be aligned with the one perceived by the real hydrophones.

The proposed approach has many advantages. First, having a spatiotemporal database that stores the noise levels produced by vessels allows to readily obtain noise maps at different time and space granularities, e.g., on a daily basis, or monthly, or seasonally. Second, the framework can be used in absence of hydrophones, which can be expensive to install and maintain, and cover a limited area. In our case study, we do calibrate the ambient noise of the model with respect to real measurements from hydrophones, but it is possible to use the model by simply assuming a reasonable value for the ambient noise. Third, it enables the distinction of contributions to underwater noise from different ship types, including not only fishing vessels but also commercial or cruise ships, provided that the AIS data are available. In this regard, we plan to acquire AIS data for all maritime traffic and, consequently, extend our analysis.

A drawback of our approach is that the boats without an AIS transceiver cannot be modelled. It is therefore not possible to estimate their contribution to the total noise, which, as a consequence, could be underestimated. This means that areas of the sea showing high values

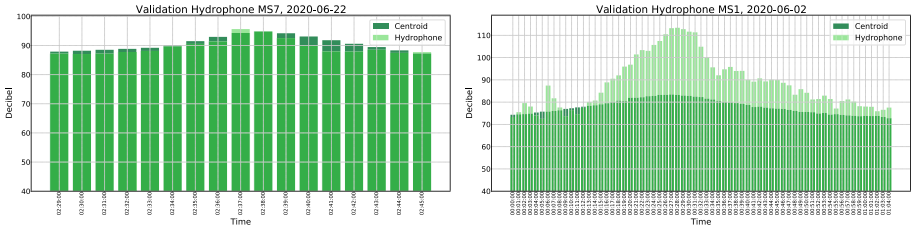

(a) June 22, 2020, from 02:29 am to 02:45 am. Hydrophone MS7 at 125 Hz.

(b) June 2, 2020, from 00:00 am to 1:04 am. Hydrophone MS1 at 125 Hz.

Fig. 11 Underwater noise measurements at different frequencies taken for each minute that a fishing vessel passes through the cell where a hydrophone is located. For each minute, the underwater noise detected by the hydrophone is represented (in light green), along with that detected by the cell centroid calculated using our model (in dark green)

of underwater noise are surely risky for the underwater world, whereas areas that result to be quiet could hide some untracked noise.

Acknowledgements We thank Fabio Pranovi for providing us the AIS data and his valuable knowledge as domain expert. We thank Elisabetta Russo for useful discussions.
This study was funded by the European Union - NextGenerationEU, in the framework of the iNEST - Interconnected Northeast Innovation Ecosystem (iNEST ECS_00000043 - CUP H43C22000540006). The second author was supported by the project "Multiscale Analysis of Human and Artificial Trajectories: Models and Applications", funded by the European Union - NextGenerationEU, Mission 4 Component 1 (MUR PRIN 2022RB939W, CUP B53D23013150006). This work took place within the framework of the DoE 2023-2027 (MUR, AIS.DIP.ECCELLENZA2023_27.FF project). The views and opinions expressed are solely those of the authors and do not necessarily reflect those of the European Union, nor can the European Union be held responsible for them.

Author Contributions GR, MS and AR have developed the initial idea. DR and GR have refined the underwater noise propagation model. EZ and GR improved the implementation in MobilityDB. GR, MS and AR have performed the analyses and GR, DR, MS and AR have interpreted the results. All the authors have contributed to the manuscript writing and have read and approved the submitted version.

Data Availability The datasets presented in this article are not available because the raw AIS data are protected by confidentiality.

Declarations

Competing interests The authors declare no competing interests.

References

1. Slabbekoorn H, Bouton N, Opzeeland I, Coers A, Cate C, Popper AN (2010) A noisy spring: the impact of globally rising underwater sound levels on fish. Trends Ecol Evol 25(7):419–427. https://doi.org/10.1016/j.tree.2010.04.005
2. Williams R, Wright AJ, Ashe E, Blight LK, Bruintjes R, Canessa R, Clark CW, Cullis-Suzuki S, Dakin DT, Erbe C, Hammond PS, Merchant ND, O'Hara PD, Purser J, Radford AN, Simpson SD, Thomas L, Wale MA (2015) Impacts of anthropogenic noise on marine life: Publication patterns, new discoveries, and future directions in research and management. Ocean Coastal Manag 115:17–24. https://doi.org/10.1016/j.ocecoaman.2015.05.021
3. MacGillivray A, McPherson C, McPherson G, Izett J, Gosselin J, Li Z, Hannay D (2014) Modelling underwater shipping noise in the Great Barrier Reef Marine Park using AIS vessel track data. In: Proceedings of the 43rd international congress on noise control engineering (Inter.noise 2014)
4. Larayedh R, Cornuelle BD, Krokos G, Hoteit I (2024) Numerical investigation of shipping noise in the Red Sea. Sci Reports 14(1):5851. https://doi.org/10.1038/s41598-024-56523-2
5. Ghezzo M, Petrizzo A, Madricardo F, Folegot T, Gallou R, Clorennec D, Chavanne R, Hemon E, Ferrarin C, Mihanović H, Pikelj K, Bastianini M, Pari A, Pari S, Menegon S, McKiver WJ, Farella G, Bosi S, Barbanti A, Picciulin M (2024) Natural and shipping underwater sound distribution in the Northern Adriatic Sea basin and possible application on target areas. Marine Pollut Bull 207:116852. https://doi.org/10.1016/j.marpolbul.2024.116852

6. Erbe C, MacGillivray A, Williams R (2012) Mapping cumulative noise from shipping to inform marine spatial planning. J Acoustical Soc Am 132(5):423–428. https://doi.org/10.1121/1.4758779
7. Neenan ST, White PR, Leighton TG, Shaw PJ (2016) Modeling vessel noise emissions through the accumulation and propagation of Automatic Identification System data. Proceed Meetings Acoust 27(1). https://doi.org/10.1121/2.0000338
8. Parent C, Spaccapietra S, Renso C, Andrienko G, Andrienko N, Bogorny V, Damiani ML, Gkoulalas-Divanis A, Macêdo JAF, Pelekis N, Theodoridis Y, Yan Z (2013) Semantic trajectories modeling and analysis. ACM Comput Surv (CSUR) 45(4):1–32. https://doi.org/10.1145/2501654.2501656
9. Mello RdS, Bogorny V, Alvares LO, Santana LHZ, Ferrero CA, Frozza AA, Schreiner GA, Renso C (2019) MASTER: A multiple aspect view on trajectories. Transact GIS 23(4):805–822. https://doi.org/10.1111/tgis.12526
10. Rovinelli G, Matwin S, Pranovi F, Russo E, Silvestri C, Simeoni M, Raffaetà A (2021) Multiple aspect trajectories: a case study on fishing vessels in the Northern Adriatic sea. In: Proceedings of the 4th international workshop on big mobility data analytics (BMDA 2021) - EDBT/ICDT Workshops, vol. 2841. https://ceur-ws.org/Vol-2841/BMDA_12.pdf
11. Brandoli B, Raffaetà A, Simeoni M, Adibi P, Bappee FK, Pranovi F, Rovinelli G, Russo E, Silvestri C, Soares A, Matwin S (2022) From multiple aspect trajectories to predictive analysis: a case study on fishing vessels in the Northern Adriatic sea. GeoInformatica 26:551–579. https://doi.org/10.1007/s10707-022-00463-4
12. Rovinelli G, Rocchesso D, Simeoni M, Raffaetà A (2024) Using semantic trajectories for spatio-temporal characterisation of underwater noise. In: Proceedings of the 6th international workshop on big mobility data analytics (BMDA 2024) - EDBT/ICDT Workshops, vol. 3651. https://ceur-ws.org/Vol-3651/BMDA-5.pdf
13. SOUNDSCAPE Project. https://www.italy-croatia.eu/web/soundscape (2019-2021)
14. Zimányi E, Sakr M, Lesuisse A (2020) MobilityDB: A mobility database based on PostgreSQL and PostGIS. ACM Trans. Database Syst 45(4). https://doi.org/10.1145/3406534
15. Chion C, Lagrois D, Dupras J (2019) A Meta-Analysis to Understand the Variability in Reported Source Levels of Noise Radiated by Ships From Opportunistic Studies. Front Marine Sci 6:714. https://doi.org/10.3389/fmars.2019.00714
16. Ainslie M (2010) Principles of Sonar Performance Modelling. Springer Praxis Books, Springer, Berlin, Heidelberg. https://doi.org/10.1007/978-3-540-87662-5
17. Geel NCF, Risch D, Wittich A (2022) A brief overview of current approaches for underwater sound analysis and reporting. Marine Pollut Bull 178:113610. https://doi.org/10.1016/j.marpolbul.2022.113610
18. Picciulin M, Petrizzo A, Madricardo F, Barbanti A, Bastianini M, Biagiotti I, Bosi S, Centurelli M, Codarin A, Costantini I, Dadić V, Falkner R, Folegot T, Galvez D, Leonori I, Menegon S, Mihanović H, Muslim S, Pari A, Pari S, Pleslić G, Radulović M, Rako-Gospić N, Sabbatini D, Tegowski J, Vukadin P, Ghezzo M (2023) First basin scale spatial-temporal characterization of underwater sound in the Mediterranean Sea. Sci Reports 13(1):22799. https://doi.org/10.1038/s41598-023-49567-3
19. Cruz E, Lloyd T, Bosschers J, Lafeber F.H, Vinagre P, Vaz G (2021) Study on inventory of existing policy, research and impacts of continuous underwater noise in Europe. In: EMSA report EMSA/NEG/21/2020. WavEC Offshore renewables and maritime research institute Netherlands
20. Erbe C, Duncan A, Hawkins L, Terhune JM, Thomas JA (2022) In: Erbe C, Thomas JA (eds.) Introduction to Acoustic Terminology and Signal Processing, Springer, Cham, pp 111–152. https://doi.org/10.1007/978-3-030-97540-1_4
21. Petrizzo A, Barfucci G, Bastianini M, Centurelli M, Codarin A, Cukrov Car M, Dadić V, Falkner R, Ghezzo M, Leonori I, Mihanović H, Muslim S, Picciulin M, Radulović M, Rako-Gospić N, Sabbatini D, VučurBlazinić T, Vukadin P, Zdroik J, Madricardo F (2022) SOUNDSCAPE North Adriatic Underwater Noise Sound Pressure Levels. https://doi.org/https://zenodo.org/records/7472152
22. Petrizzo A, Barbanti A, Barfucci G, Bastianini M, Biagiotti I, Bosi S, Centurelli M, Chavanne R, Codarin A, Costantini I, Cukrov Car M, Dadić V, Falcieri FM, Falkner R, Farella G, Felli M, Ferrarin C, Folegot T, Gallou R, Galvez D, Ghezzo M, Kruss A, Leonori I, Menegon S, Mihanović H, Muslim S, Pari A, Pari S, Picciulin M, Pleslić G, Radulović M, Rako-Gospić N, Sabbatini D, Soldano G, Tęgowski J, Vučur-Blazinić T, Vukadin P, Zdroik J, Madricardo F (2023) First assessment of underwater sound levels in the Northern Adriatic Sea at the basin scale. Sci Data 10(1):137. https://doi.org/10.1038/s41597-023-02033-1
23. Diviacco P, Nadali A, Iurcev M, Burca M, Carbajales R, Gangale M, Busato A, Brunetti F, Grio L, Viola A, Potleca N (2021) Underwater Noise Monitoring with Real-Time and Low-Cost Systems, (The CORMA Experience). J Marine Sci Eng 9(4):390. https://doi.org/10.3390/jmse9040390

24. Moran K, Boutin B, Juniper SK, Pirenne B, Round A (2019) A multi-use and multi-stakeholder ocean observing platform system. In: OCEANS 2019 MTS/IEEE SEATTLE, pp 1–5. https://doi.org/10.23919/OCEANS40490.2019.8962711
25. Farcas A, Powell CF, Brookes KL, Merchant ND (2020) Validated shipping noise maps of the Northeast Atlantic. Sci Total Environ 735:139509. https://doi.org/10.1016/j.scitotenv.2020.139509
26. Picciulin M, Facca C, Fiorin R, Riccato F, Zucchetta M, Malavasi S (2021) It Is Not Just a Matter of Noise: Sciaena umbra Vocalizes More in the Busiest Areas of the Venice Tidal Inlets. J Marine Sci Eng 9(2):237. https://doi.org/10.3390/jmse9020237
27. MacGillivray A, Jong C (2021) A Reference Spectrum Model for Estimating Source Levels of Marine Shipping Based on Automated Identification System Data. J Marine Sci Eng 9(4):369. https://doi.org/10.3390/jmse9040369
28. SAS QO Quonops online services. http://qos.quiet-oceans.com/
29. Jalkanen J-P, Johansson L, Andersson MH, Majamäki E, Sigray P (2022) Underwater noise emissions from ships during 2014–2020. Environ Pollut 311:119766. https://doi.org/10.1016/j.envpol.2022.119766
30. Johansson L, Jalkanen J-P, Kukkonen J (2017) Global assessment of shipping emissions in 2015 on a high spatial and temporal resolution. Atmos Environ 167:403–415. https://doi.org/10.1016/j.atmosenv.2017.08.042
31. Farcas A, Thompson PM, Merchant ND (2016) Underwater noise modelling for environmental impact assessment. Environ Impact Assess Rev 57:114–122. https://doi.org/10.1016/j.eiar.2015.11.012
32. Urick RJ (1983) Principles of underwater sound 3rd edition. Peninsula Publising Los Atlos, California 22:23–24
33. Etter PC (2013) Underwater Acoustic Modeling and Simulation, 4th edition edn., pp 554. CRC Press, Boca Raton. https://doi.org/10.1201/b13906
34. Rogers PH, Cox M (1988) Underwater sound as a biological stimulus. In: Atema J, Fay RR, Popper AN, Tavolga WN (eds.) Sensory Biology of Aquatic Animals, pp 131–149. Springer, New York, NY. https://doi.org/10.1007/978-1-4612-3714-3_5
35. Richardson WJ, Greene CR Jr, Malme CI, Thomson DH (1995) Marine Mammals and Noise. Academic Press, London, UK. https://doi.org/10.1016/C2009-0-02253-3
36. De Robertis A, Wilson CD (2006) Walleye pollock respond to trawling vessels. ICES J Marine Sci 63(3):514–522. https://doi.org/10.1016/j.icesjms.2005.08.014
37. Mitson R (1993) Underwater noise radiated by research vessels. ICES Marine science symposium 196:147–152
38. Erbe C, Duncan A, Vigness-Raposa KJ (2022) In: Erbe C, Thomas JA (eds.) Introduction to Sound Propagation Under Water, pp 185–216. Springer, Cham. https://doi.org/10.1007/978-3-030-97540-1_6
39. Oliveira TC, Lin Y-T, Porter MB (2021) Underwater sound propagation modeling in a complex shallow water environment. Front Marine Sci 8:751327. https://doi.org/10.3389/fmars.2021.751327
40. Smith TA, Kourounioti M (2023) Underwater radiated noise from small vessels in shallow water: propagation modelling and experimental measurements. Conference Proceedings of INEC. https://doi.org/10.24868/10687
41. Francois R, Garrison G (1982) Sound absorption based on ocean measurements: Part I: Pure water and magnesium sulfate contributions. J Acoustical Soc Am 72(3):896–907. https://doi.org/10.1121/1.388170
42. Rovinelli G, Zimányi E, Simeoni M, Rocchesso D, Raffaetà A (2025) A Scalable Model for Vessel-Generated Underwater Noise: Enhancing Efficiency through Parallelisation. In: Proceedings of the 7th international workshop on big mobility data analytics (BMDA 2025) - EDBT/ICDT Workshops
43. Russo E, Anelli Monti M, Toninato G, Silvestri C, Raffaetà A, Pranovi F (2021) Lockdown: How the COVID-19 pandemic affected the fishing activities in the Adriatic Sea (Central Mediterranean Sea). Front Marine Sci 8:685808. https://doi.org/10.3389/fmars.2021.685808
44. Folegot T, Hemon E, Nehls G, Schmiing M, Bräger S, Bellmann M, Gerlach S, Matuschek R, Flamme J (2024) In: Popper AN, Sisneros J, Hawkins AD, Thomsen F (eds.) Near Real-Time Underwater Sound Modeling of Dredging Noise to Meet Regulatory Noise Thresholds, pp 1–19. Springer, Cham. https://doi.org/10.1007/978-3-031-10417-6_52-1

Giulia Rovinelli received her M.Sc. in Computer Science from Ca' Foscari University of Venice (Italy) in 2022. She is currently a PhD student in Computer Science at Ca' Foscari University of Venice (Italy). Her research focuses on data mining, spatiotemporal and mobility databases, and semantic trajectory modelling and analysis.

Davide Rocchesso received the Ph.D. degree from the University of Padova, Italy in 1996. He is professor of computer science at the University of Milan, Italy. He was the coordinator of EU projects SOb (the Sounding Object) and SkAT-VG (Sketching Audio Technologies using Vocalizations and Gestures). He had been chairing the COST Action on Sonic Interaction Design. His main research interests are sound modelling and synthesis, interaction design, evaluation of multisensory interactions.

Marta Simeoni received her PhD in Computer Science in 2000 from the University of Rome "La Sapienza". Since 2000 she is assistant professor at Ca' Foscari University of Venice. Her current research interests include bioinformatics and modelling and analysis of biological and ecological systems. Recent research interests include also modelling and analysing semantic trajectories.

Esteban Zimányi is a professor at the Université libre de Bruxelles (ULB). He started his studies at the Universidad Autónoma de Centro América, Costa Rica, and received a Master in Computer Science degree and a doctorate in computer science from ULB. His current research interests include spatiotemporal and mobility databases, data warehouses, and geographic in formation systems. He has coauthored and coedited several books and published many papers on these topics. He was editor-in-chief of the Journal on Data Semantics (JoDS) published by Springer from 2012 to 2020. He is the coordinator of the Erasmus Mundus master's and doctorate programs "Information Technologies for Business Intelligence" (IT4BI) and "Big Data Management and Analytics" (BDMA), and the Marie Skłodowska-Curie doctorate program "Data Engineering for Data Science" (DEDS). He is a main contributor and a co-founder of MobilityDB.

Alessandra Raffaetà MSc (1994) and PhD (2000) in Computer Science, University of Pisa - is an assistant professor at Ca' Foscari University of Venice (Italy). Her research interests include Data warehouses, GISs, spatiotemporal reasoning, design and formal semantics of programming languages and mobility data analytics. She published over 70 papers on international journals and conferences. She was member of the program committee of several international conferences and she participated to several national and international research projects.